

*RUNNING HEAD: Networks across human menstrual cycle*

## **Functional reorganization of brain networks across the human menstrual cycle**

Laura Pritschet<sup>1\*</sup>, Tyler Santander<sup>1\*</sup>, Evan Layher<sup>1</sup>, Caitlin M. Taylor<sup>1</sup>, Shuying Yu<sup>1</sup>, Michael B. Miller<sup>1,2,3</sup>, Scott T. Grafton<sup>1,2</sup>, & Emily G. Jacobs<sup>1,3</sup>

<sup>1</sup>Department of Psychological & Brain Sciences, University of California, Santa Barbara, Santa Barbara, CA

<sup>2</sup> Institute for Collaborative Biotechnologies, University of California, Santa Barbara, Santa Barbara, CA

<sup>3</sup>Neuroscience Research Institute, University of California, Santa Barbara, Santa Barbara, CA

\*Authors contributed equally to this work.

### **Correspondence:**

Emily G. Jacobs

Department of Psychological & Brain Sciences

University of California, Santa Barbara

Santa Barbara, CA 93106

[emily.jacobs@psych.ucsb.edu](mailto:emily.jacobs@psych.ucsb.edu)

**Key Words:** sex hormones | estrogen | progesterone | functional connectivity | resting-state

## 1 Abstract

2 The brain is an endocrine organ, sensitive to the rhythmic changes in sex hormone  
3 production that occurs in most mammalian species. In rodents and nonhuman primates,  
4 estrogen and progesterone's impact on the brain is evident across a range of  
5 spatiotemporal scales. Yet, the influence of sex hormones on the functional architecture of  
6 the human brain is largely unknown. In this dense-sampling, deep phenotyping study, we  
7 examine the extent to which endogenous fluctuations in sex hormones alter intrinsic brain  
8 networks at rest in a woman who underwent brain imaging and venipuncture for 30  
9 consecutive days. Standardized regression analyses illustrate estrogen and progesterone's  
10 widespread influence on cortical dynamics. Time-lagged analyses examined the  
11 directionality of these relationships and reveal estrogen's ability to drive connectivity  
12 across major functional brain networks, including the Default Mode and Dorsal Attention  
13 Networks, whose hubs are densely populated with estrogen receptors. These results  
14 reveal the rhythmic nature in which brain networks reorganize across the human  
15 menstrual cycle. Neuroimaging studies that densely sample the individual connectome  
16 have begun to transform our understanding of the brain's functional organization. As  
17 these results indicate, taking endocrine factors into account is critical for fully  
18 understanding the intrinsic dynamics of the human brain.

19

## Introduction

20 The brain is an endocrine organ whose day-to-day function is intimately tied to the action  
21 of neuromodulatory hormones<sup>1–4</sup>. Yet, the study of brain-hormone interactions in human  
22 neuroscience has often been woefully myopic in scope: the classical approach of  
23 interrogating the brain involves collecting data at a single time point from multiple  
24 subjects and averaging across individuals to provide evidence for a  
25 hormone-brain-behavior relationship. This cross-sectional approach obscures the rich,  
26 rhythmic nature of endogenous hormone production. A promising trend in network  
27 neuroscience is to flip the cross-sectional model by tracking small samples of individuals  
28 over timescales of weeks, months, or years to provide insight into how biological,  
29 behavioral, and state-dependent factors influence intra- and inter-individual variability in  
30 the brain's intrinsic network organization<sup>5–7</sup>. Neuroimaging studies that densely sample  
31 the individual connectome are beginning to transform our understanding of the dynamics  
32 of human brain organization. However, these studies commonly overlook sex steroid  
33 hormones as a source of variability—a surprising omission given that sex hormones are  
34 powerful neuromodulators that display stable circadian, infradian, and circannual  
35 rhythms in nearly all mammalian species. In the present study, we illustrate robust,  
36 time-dependent interactions between the sex steroid hormones 17 $\beta$ -estradiol and  
37 progesterone and the functional network organization of the brain over a complete  
38 menstrual cycle, offering compelling evidence that sex hormones drive widespread  
39 patterns of connectivity in the human brain.

40 Converging evidence from rodent<sup>1,2,8</sup>, non-human primate<sup>9,10</sup>, and human  
41 neuroimaging studies<sup>11-16</sup> has established the widespread influence of 17 $\beta$ -estradiol and  
42 progesterone on regions of the mammalian brain that support higher level cognitive  
43 functions. Estradiol and progesterone signaling are critical components of cell survival  
44 and plasticity, exerting excitatory and inhibitory effects that are evident across multiple  
45 spatial and temporal scales<sup>4,8</sup>. The dense expression of estrogen and progesterone  
46 receptors (ER; PR) in cortical and subcortical tissue underscores the widespread nature of  
47 hormone action. For example, in non-human primates ~50% of pyramidal neurons in  
48 prefrontal cortex (PFC) express ER<sup>10</sup> and estradiol regulates dendritic spine proliferation  
49 in this region<sup>3</sup>. In rodents, fluctuations in estradiol across the estrous cycle enhance  
50 spinogenesis in hippocampal CA1 neurons and progesterone inhibits this effect<sup>1</sup>.

51 During an average human menstrual cycle, occurring every 25-32 days, women  
52 experience a ~12-fold increase in estradiol and an ~800-fold increase in progesterone.  
53 Despite this striking change in endocrine status, we lack a complete understanding of how  
54 the large-scale functional architecture of the human brain responds to rhythmic changes in  
55 sex hormone production across the menstrual cycle. Much of our understanding of  
56 cycle-dependent changes in brain structure<sup>1,17</sup> and function<sup>18-20</sup> comes from rodent  
57 studies, since the length of the human menstrual cycle (at least 5 $\times$  longer than rodents')  
58 presents experimental hurdles that make longitudinal studies challenging. A common  
59 solution is to study women a few times throughout their cycle, targeting stages that  
60 roughly correspond to peak/trough hormone concentrations. Using this 'sparse-sampling'

61 approach, studies have examined resting-state connectivity in discrete stages of the  
62 cycle<sup>13,14,21-23</sup>; however, some of these findings are undermined by inconsistencies in cycle  
63 staging methods, lack of direct hormone assessments, or limitations in functional  
64 connectivity methods.

65 In this dense-sampling, deep-phenotyping study, we assessed brain-hormone  
66 interactions over 30 consecutive days representing a complete menstrual cycle. Our  
67 results reveal that intrinsic functional connectivity is influenced by hormone dynamics  
68 across the menstrual cycle at multiple spatiotemporal resolutions. Estradiol and  
69 progesterone conferred robust time-synchronous and time-lagged effects on the brain,  
70 demonstrating that intrinsic fluctuations in sex hormones drive changes in the functional  
71 network architecture of the human brain. Together, these findings provide insight into  
72 how brain networks reorganize across the human menstrual cycle and suggest that  
73 consideration of the hormonal milieu is critical for fully understanding the intrinsic  
74 dynamics of the human brain.

## 75 **Results**

76 A healthy, naturally-cycling female (author L.P.; age 23) underwent venipuncture and MRI  
77 scanning for 30 consecutive days. The full dataset consists of daily mood, diet, physical  
78 activity, and behavioral assessments; task-based and resting-state fMRI; structural MRI;  
79 and serum assessments of pituitary gonadotropins and ovarian sex hormones.

80 Neuroimaging data, analysis code, and daily behavioral assessments will be publicly  
81 accessible upon publication.

**Table 1.** Gonadal and pituitary hormones by cycle stage.

	<b>Follicular</b>	<b>Ovulatory</b>	<b>Luteal</b>
	Mean (SD) <i>standard range</i>	Mean (SD) <i>standard range</i>	Mean (SD) <i>standard range</i>
Estradiol (pg/mL)	37.9 (15.9) 12.5–166.0	185.3 (59.0) 85.8–498.0	85.4 (26.4) 43.8–210.0
Progesterone (ng/mL)	0.2 (0.2) 0.1–0.9	0.2 (0.2) 0.1–120	9.5 (4.8) 1.8–23.9
LH (mIU/mL)	5.9 (0.7) 2.4–12.6	21.7 (16.4) 14.0–95.6	5.5 (2.0) 1.0–11.4
FSH (mIU/mL)	6.5 (1.2) 3.5–12.5	8.1 (3.6) 4.7–21.5	4.8 (1.3) 1.7–7.7

*Note.* Standard reference ranges based on aggregate data from Labcorp (<https://www.labcorp.com/>).

## 82 **Endocrine assessments**

83 Analysis of daily sex hormone (by liquid-chromatography mass-spectrometry; LC-MS)  
84 and gonadotropin (by chemiluminescent immunoassay) concentrations confirmed the  
85 expected rhythmic changes of a typical menstrual cycle, with a total cycle length of 27  
86 days. Serum levels of estradiol and progesterone were lowest during menses (day 1–4) and  
87 peaked in late follicular (estradiol) and late luteal (progesterone) phases (Figure 1; Table  
88 1). Progesterone concentrations surpassed 5 ng/mL in the luteal phase, signaling an  
89 ovulatory cycle<sup>24</sup>.

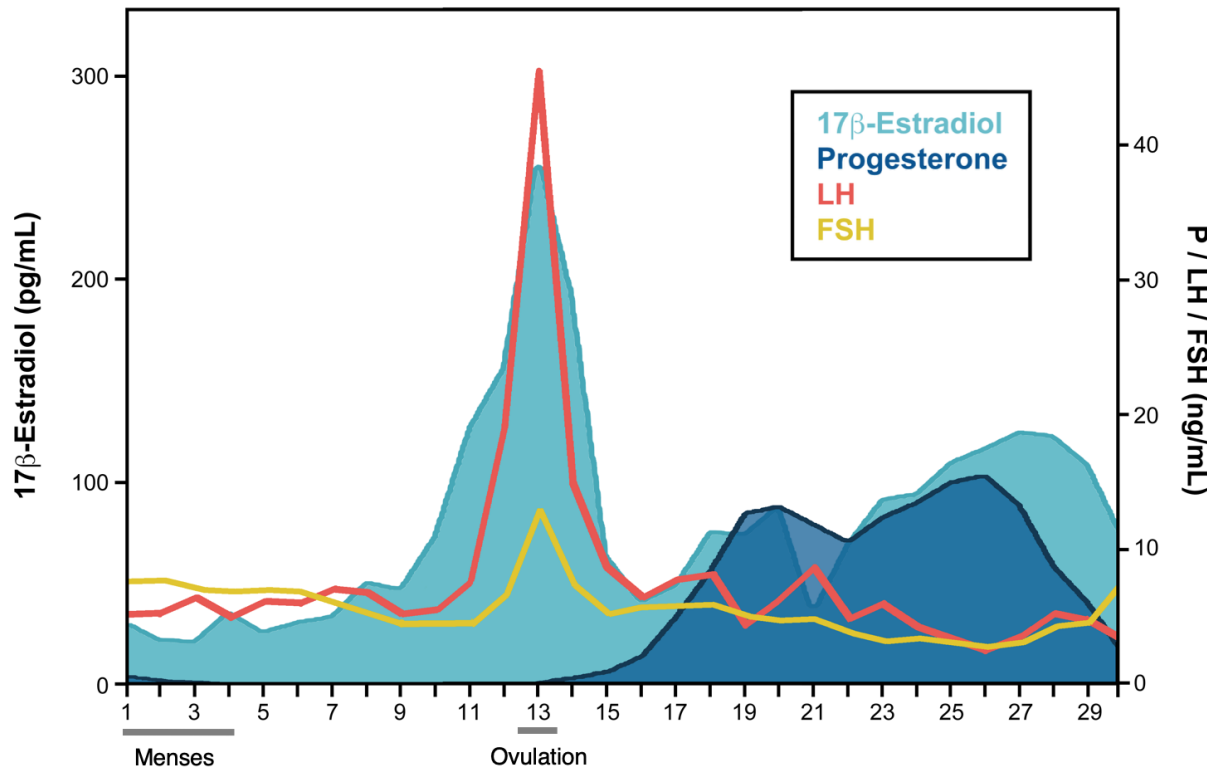


**Figure 1. Participant's hormone concentrations plotted by day of cycle.**  $17\beta$ -estradiol, progesterone, luteinizing hormone (LH), and follicle stimulating hormone (FSH) concentrations fell within standard ranges.

90 **Time-synchronous associations between sex hormones and**  
91 **whole-brain functional connectivity**

92 To begin, we tested the hypothesis that whole-brain functional connectivity at rest is  
93 associated with intrinsic fluctuations in estradiol and progesterone in a *time-synchronous*  
94 (i.e. day-by-day) fashion. Based on the enriched expression of ER in PFC<sup>10</sup>, we predicted  
95 that the Default Mode, Frontoparietal Control, and Dorsal Attention Networks would be  
96 most sensitive to hormone fluctuations across the cycle. For each session, the brain was  
97 parcellated into 400 cortical regions from the Schaefer atlas<sup>25</sup> and 15 subcortical regions  
98 from the Harvard-Oxford atlas (Figure 2C). A summary time-course was extracted from

99 each parcel, data were temporally-filtered using a maximal overlap discrete wavelet  
100 transform (scales 3–6;  $\sim$ 0.01–0.17 Hz), and  $415 \times 415$  functional association matrices were  
101 constructed via magnitude-squared coherence (FDR-thresholded at  $q < .05$ ; see **Methods**  
102 and **Materials** for a full description of preprocessing and connectivity estimation). Next,  
103 we specified edgewise regression models, regressing coherence against estradiol and  
104 progesterone over the 30 days of the study. All data were  $Z$ -scored prior to analysis and  
105 models were thresholded against empirical null distributions generated through 10,000  
106 iterations of nonparametric permutation testing. Results reported below survived a  
107 conservative threshold of  $p < .001$ .

108 We observed robust increases in coherence as a function of increasing estradiol across  
109 the brain (**Figure 2A**). When summarizing across networks (computing the mean  
110 association strength across network nodes, where strength was defined per graph theory  
111 as the sum of positive and negative edge weights linked to each node, independently),  
112 components of the Temporal Parietal Network had the strongest positive associations on  
113 average, as well as the most variance (**Figure 2D**). With the exception of Subcortical nodes,  
114 all networks demonstrated some level of significantly positive association strength (95%  
115 CIs not intersecting zero). We observed a paucity of edges showing inverse associations  
116 (connectivity decreasing while estradiol increased), with no networks demonstrating  
117 significantly negative association strengths on average. These findings suggest that  
118 edgewise functional connectivity is primarily characterized by increased coupling as  
119 estradiol rises over the course of the cycle.

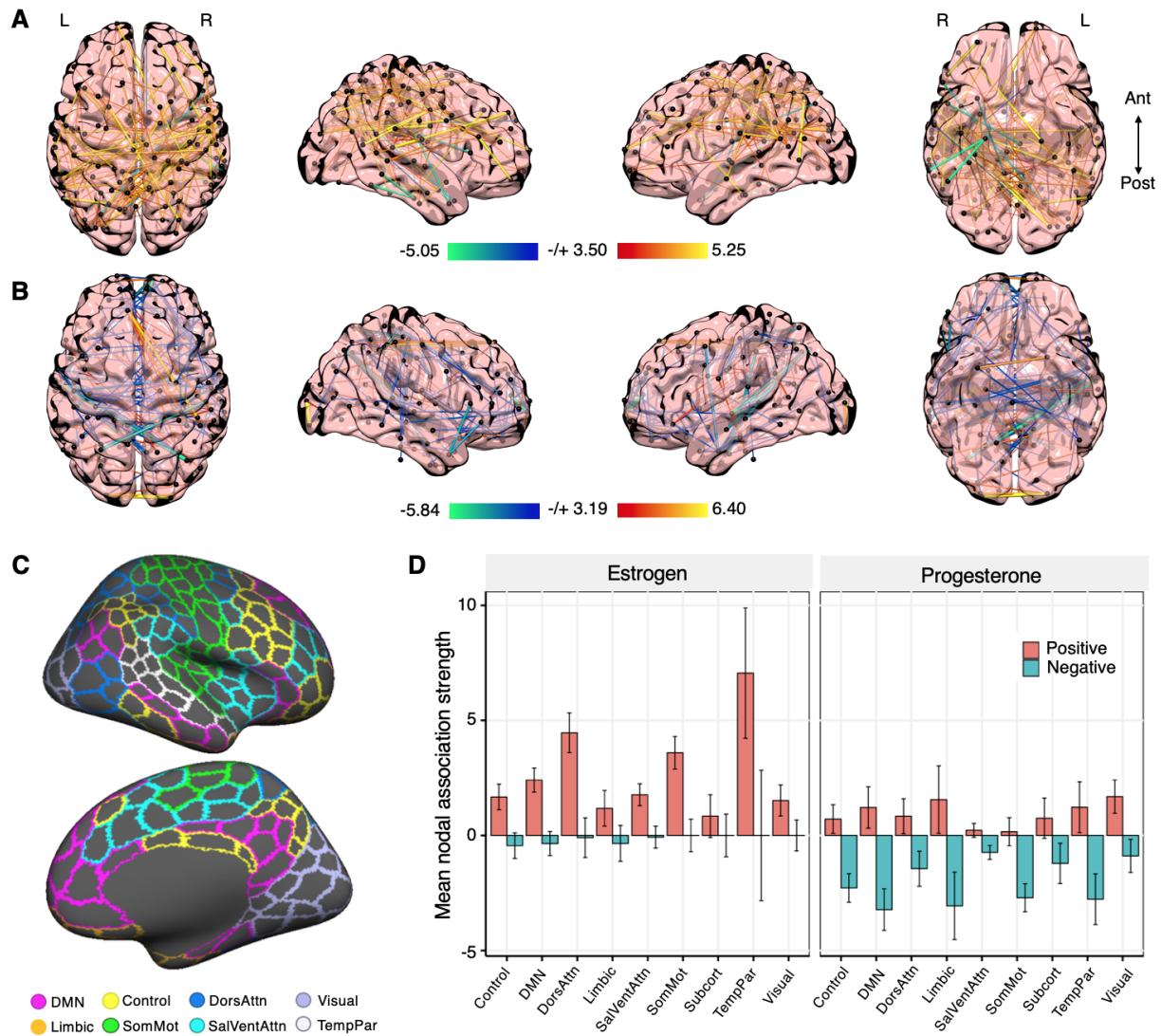


**Figure 2. Whole-brain functional connectivity at rest is associated with intrinsic fluctuations in estradiol and progesterone.** (A) Time-synchronous (i.e. day-by-day) associations between estradiol and coherence. Hotter colors indicate increased coherence with higher concentrations of estradiol; cool colors indicate the reverse. Results are empirically-thresholded via 10,000 iterations of nonparametric permutation testing ( $p < .001$ ). Nodes without significant edges are omitted for clarity. (B) Time-synchronous associations between progesterone and coherence. (C) Cortical parcellations were defined by the 400-node Schaefer atlas (shown here). An additional 15 subcortical nodes were defined from the Harvard-Oxford atlas. (D) Mean nodal association strengths by network and hormone. Error bars give 95% confidence intervals. Abbreviations: DMN, Default Mode Network; DorsAttn, Dorsal Attention Network; SalVentAttn, Salience/Ventral Attention Network; SomMot, SomatoMotor Network; TempPar, Temporal Parietal Network.

120 Progesterone, by contrast, yielded a widespread pattern of inverse association across  
121 the brain, such that connectivity decreased as progesterone rose (**Figure 2B**). Most  
122 networks (with the exception of the Salience/Ventral Attention and SomatoMotor  
123 Networks) still yielded some degree of significantly positive association over time;  
124 however, the general strength of negative associations was larger in magnitude and  
125 significantly nonzero across all networks (**Figure 2D**). Together, these results align with  
126 animal models suggesting excitatory and inhibitory roles for estradiol and progesterone,  
127 respectively, manifested here as predominant increases and decreases in functional  
128 connectivity across the cycle.

129 **Time-lagged associations between estradiol and whole-brain functional  
130 connectivity**

131 We then employed time-lagged methods from dynamical systems analysis to further  
132 elucidate the influence of hormonal fluctuations on intrinsic functional connectivity:  
133 specifically, vector autoregression (VAR), which supports more directed, causal inference  
134 than standard regression models. Here we chose to focus exclusively on estradiol for two  
135 reasons: 1) the highly-bimodal time-course of progesterone confers a considerably longer  
136 autocorrelative structure, requiring many more free parameters (i.e. higher-order models,  
137 ultimately affording fewer degrees of freedom); and 2) progesterone lacks an appreciable  
138 pattern of periodicity in its autocovariance with network timeseries, suggesting less  
139 relevance for time-lagged analysis over a single cycle. In contrast, estradiol has a much  
140 smoother time-course that is well-suited for temporal-evolution models such as VAR.

141 In short, VAR solves a simultaneous system of equations that predicts *current* states of  
142 the brain and estradiol from the *previous* states of each. We report results from  
143 second-order VAR models: thus, in order to predict connectivity or hormonal states on a  
144 given day of the experiment, we consider their values on both the previous day (hereafter  
145 referred to as 'lag 1') and two days prior (hereafter referred to as 'lag 2'). See **Methods**  
146 and **Materials** for an additional mathematical description. Ultimately, if brain variance  
147 over time is attributable to previous states of estradiol, this suggests that temporal  
148 dynamics in connectivity may be *driven* (in part) by fluctuations in hormonal states. Vector  
149 autoregressive models were specified for each network edge; as before, all data were  
150  $Z$ -scored and models were empirically thresholded against 10,000 iterations of  
151 nonparametric permutation testing. Surviving edges were significant at the  $p < .001$  level.

152 When predicting edgewise connectivity states, a powerful disparity emerged between  
153 the brain's autoregressive effects and the effects of estradiol. We observed vast,  
154 whole-brain associations with prior hormonal states, both at lag 1 and lag 2 (**Figure 3A**).  
155 Perhaps most immediately striking, the sign of these brain-hormone associations inverts  
156 between lags, such that it is predominantly positive at lag 1 and predominantly negative  
157 at lag 2—this holds for all networks when considering their nodal association strengths  
158 (**Figure 3B**). We interpret this as a potential regulatory dance between brain states and  
159 hormones over the course of the cycle, with estradiol perhaps playing a role in  
160 maintaining both steady states (when estradiol is low) and transiently-high dynamics  
161 (when estradiol rises). No such pattern emerged in the brain's autoregressive effects, with

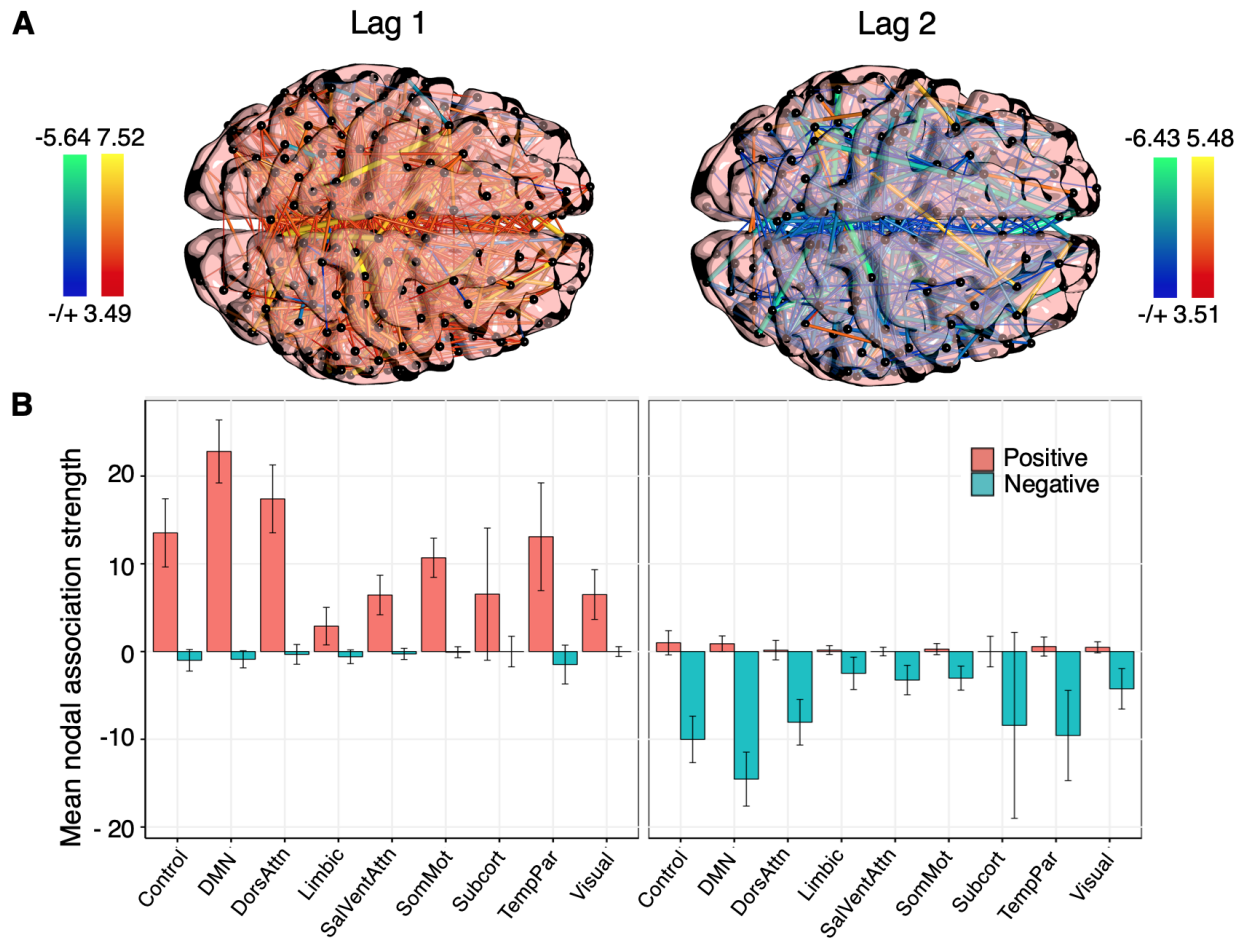


**Figure 3. Whole-brain functional connectivity is linearly dependent on previous states of estradiol.** (A) Time-lagged associations between coherence and estradiol at lag 1 (left) and lag 2 (right), derived from edgewise vector autoregression models. Hotter colors indicate a predicted increase in coherence given previous concentrations of estradiol; cool colors indicate the reverse. Results are empirically-thresholded via 10,000 iterations of nonparametric permutation testing ( $p < .001$ ). Nodes without significant edges are omitted for clarity. (B) Mean nodal association strengths by network and time lag. Error bars give 95% confidence intervals.

<sup>162</sup> sparse, low-magnitude, and predominantly negative associations at lag 1 and lag 2  
<sup>163</sup> (**Supplementary Figure 1**). The flow of effect between estradiol and edgewise  
<sup>164</sup> connectivity was partially unidirectional. Previous states of coherence predicted estradiol  
<sup>165</sup> across a number of edges, intersecting all brain networks. This emerged at both lag 1 and  
<sup>166</sup> lag 2; however, unlike the lagged effects of estradiol on coherence, association strengths  
<sup>167</sup> were predominantly negative and low-magnitude (on average) at both lags  
<sup>168</sup> (**Supplementary Figure 2**). Moreover—and importantly—none of the edges that *predicted*  
<sup>169</sup> estradiol were also significantly predicted *by* estradiol at either lag (i.e. there was no  
<sup>170</sup> evidence of mutual modulation at any network edge).

<sup>171</sup> **Time-lagged associations between estradiol and functional network  
172 topologies**

<sup>173</sup> Given the findings above, we applied the same time-lagged framework to *topological states*  
<sup>174</sup> of brain networks in order to better capture the directionality and extent of brain-hormone  
<sup>175</sup> interactions at the network level. These states were quantified using common graph  
<sup>176</sup> theory metrics: namely, the *participation coefficient* (an estimate of *between-network*  
<sup>177</sup> integration) and *global efficiency* (an estimate of *within-network* integration). As before, all  
<sup>178</sup> data were *Z*-scored prior to VAR estimation, and model parameters/fit were compared  
<sup>179</sup> against 10,000 iterations of nonparametric permutation testing. We focus on significant  
<sup>180</sup> network-level effects below, but a full documentation of our findings is available in  
<sup>181</sup> **Supplementary Tables 1 and 2.**

**Table 2.** VAR model fit: Between-network participation.

Network	Outcome	Predictor	Estimate	SE	<i>T</i> ( <i>p</i> )
Participation	Dorsal Attention	Constant	0.08	0.16	0.49 (.099)
		DAN <sub><i>t-1</i></sub>	0.15	0.18	0.84 (.405)
		<b>Estradiol<sub><i>t-1</i></sub></b>	<b>-0.56</b>	<b>0.25</b>	<b>-2.27 (.035)</b>
		DAN <sub><i>t-2</i></sub>	-0.29	0.17	-1.71 (.093)
		<b>Estradiol<sub><i>t-2</i></sub></b>	<b>0.53</b>	<b>0.24</b>	<b>2.16 (.042)</b>
<i>R</i> <sup>2</sup> = 0.32 ( <i>p</i> = .049); RMSE = 0.79 ( <i>p</i> = .050)					
Estradiol	Dorsal Attention	Constant	6.88 × 10 <sup>-5</sup>	0.12	0.001 (.998)
		DAN <sub><i>t-1</i></sub>	0.06	0.14	0.47 (.627)
		<b>Estradiol<sub><i>t-1</i></sub></b>	<b>1.12</b>	<b>0.18</b>	<b>6.12 (&lt;.0001)</b>
		DAN <sub><i>t-2</i></sub>	0.03	0.13	0.24 (.806)
		<b>Estradiol<sub><i>t-2</i></sub></b>	<b>-0.48</b>	<b>0.18</b>	<b>-2.65 (.007)</b>
<i>R</i> <sup>2</sup> = 0.67 ( <i>p</i> = .0001); RMSE = 0.59 ( <i>p</i> = .0009)					

*Note.* *p*-values empirically-derived via 10,000 iterations of nonparametric permutation testing.

<sup>182</sup> **Estradiol and between-network participation**

<sup>183</sup> As expected, estradiol demonstrated significant autoregressive effects across all models.

<sup>184</sup> Previous states of estradiol also significantly predicted between-network integration

<sup>185</sup> across several intrinsic networks; however, overall model fit (variance accounted for, *R*<sup>2</sup>,

<sup>186</sup> and root mean-squared error, *RMSE*) was at best marginal compared to empirical null

<sup>187</sup> distributions of these statistics. For example, in the Dorsal Attention Network (DAN;

<sup>188</sup> **Figure 4A-B; Table 2**), estradiol was a significant predictor of between-network

<sup>189</sup> participation both at lag 1 (*b* = -0.56, *SE* = 0.25, *t* = -2.27, *p* = .035) and at lag 2

<sup>190</sup> (*b* = 0.53, *SE* = 0.24, *t* = 2.16, *p* = .042). Overall fit for DAN participation, however,

<sup>191</sup> rested at the classical frequentist threshold for significance, relative to empirical nulls

<sup>192</sup> (*R*<sup>2</sup> = 0.32, *p* = .049; *RMSE* = 0.79, *p* = .050). We observed a similar pattern of results for

193 the Default Mode Network (DMN) and Limbic Network, where lagged states of estradiol  
194 significantly predicted cross-network participation, but model fit as a whole was low (see  
195 **Supplementary Table 1**). Interestingly, for all three of these networks, there were no  
196 significant autoregressive effects of brain states—previous states of network participation  
197 also did not predict estradiol, suggesting that modulation of network topology likely goes  
198 from hormones to brain, not the other way around.

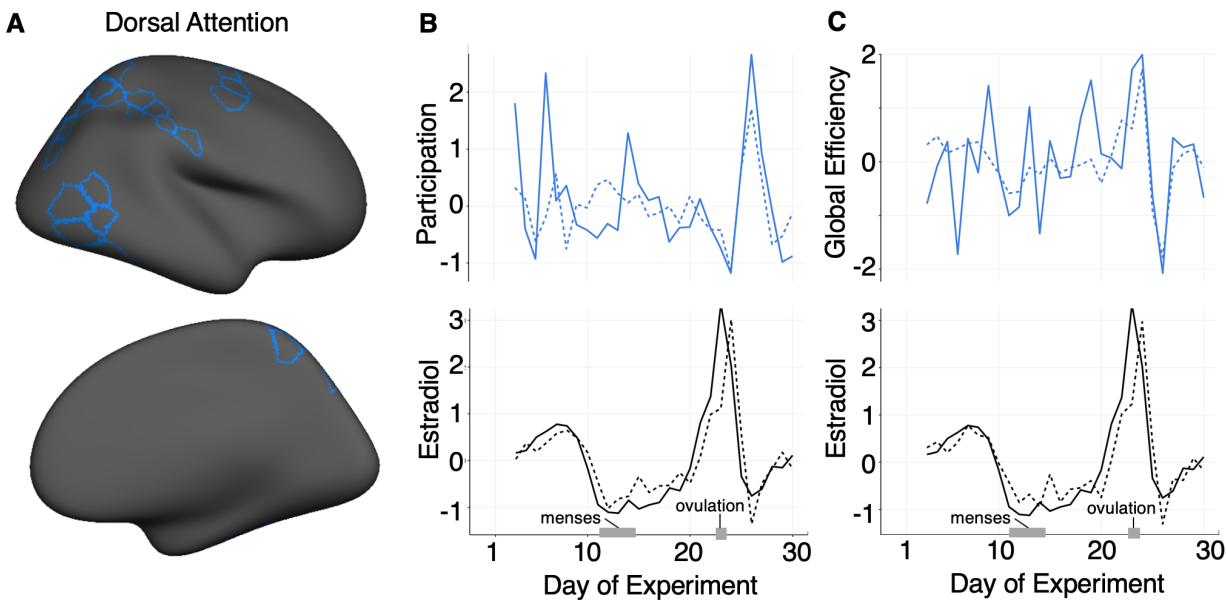


**Figure 4. Dorsal Attention Network topology is driven by previous states of estradiol.** Observed data (solid lines) vs. VAR model fits (dotted lines) for between-network participation (B, middle) and within-network efficiency (C, right) in the Dorsal Attention Network (A, left). Timeseries for each network statistic are depicted above in (B,C) and estradiol for each VAR is plotted below. Data are in standardized units and begin at experiment day three, given the second-order VAR (lag of two days).

199 The single exception to this trend was the Visual Network. Prediction of its  
200 between-network participation yielded a significant model fit ( $R^2 = 0.37, p = .024$ ;  
201  $RMSE = 0.79, p = .044$ ). However, this was primarily driven by autoregressive effects of  
202 the network at lag 1 ( $b = -0.39, SE = 0.17, t = -2.30, p = .027$ ) and lag 2 ( $b = -0.43$ ,

203  $SE = 0.17, t = -2.46, p = .024$ ); estradiol yielded a marginal (but nonsignificant) effect  
204 only at lag 2 ( $b = 0.49, SE = 0.24, t = 2.01, p = .058$ ).

205 **Estradiol and global efficiency**

206 In contrast to between-network integration, estradiol was a strong predictor of  
207 within-network integration, both in terms of parameter estimates and overall fit. Here, the  
208 Default Mode Network provided the best-fitting model ( $R^2 = 0.50, p = .003$ ;  
209  $RMSE = 0.70, p = .022$ ; **Figure 5A-B**). As before, estradiol demonstrated significant  
210 autoregressive effects at lag 1 ( $b = 1.15, SE = 0.19, t = 6.15, p < .0001$ ) and lag 2  
211 ( $b = -0.48, SE = 0.19, t = -2.50, p = .012$ ). When predicting DMN efficiency, previous  
212 states of estradiol remained significant both at lag 1 ( $b = 0.98, SE = 0.23, t = 3.37$ ,  
213  $p = .0003$ ) and at lag 2 ( $b = -0.93, SE = 0.23, t = -4.00, p = .002$ ). Critically, these effects  
214 were purely directional: prior states of Default Mode efficiency did not predict estradiol,  
215 nor did they have significant autoregressive effects, supporting the conclusion that  
216 variance in topological network states (perhaps within-network integration, in particular)  
217 is primarily accounted for by estradiol—not the other way around (**Table 3**).

218 We observed a similar pattern of results in the Dorsal Attention Network ( $R^2 = 0.37$ ,  
219  $p = .022; RMSE = 0.77, p = .023$ ; **Figure 4C; Table 3**). Estradiol again demonstrated  
220 significant autoregressive effects at lag 1 ( $b = 1.17, SE = 0.19, t = 6.30, p < .0001$ ) and lag  
221 2 ( $b = -0.48, SE = 0.19, t = -2.49, p = .011$ ), along with predicting DAN efficiency both  
222 at lag 1 ( $b = 0.84, SE = 0.25, t = 3.35, p = .002$ ) and at lag 2 ( $b = -0.67, SE = 0.16$ ,

**Table 3.** VAR model fit: Global efficiency.

Network	Outcome	Predictor	Estimate	SE	<i>T</i> ( <i>p</i> )
Efficiency	Default Mode	Constant	0.04	0.15	0.28 (.279)
		DMN <sub><i>t-1</i></sub>	-0.04	0.16	-0.27 (.764)
		<b>Estradiol<sub><i>t-1</i></sub></b>	<b>0.98</b>	<b>0.23</b>	<b>3.37 (.0003)</b>
		DMN <sub><i>t-2</i></sub>	-0.02	0.16	-0.11 (.907)
		<b>Estradiol<sub><i>t-2</i></sub></b>	<b>-0.93</b>	<b>0.23</b>	<b>-4.00 (.002)</b>
<i>R</i> <sup>2</sup> = 0.50 ( <i>p</i> = .003); RMSE = 0.70 ( <i>p</i> = .022)					
Estradiol	Dorsal Attention	Constant	0.01	0.12	0.09 (.729)
		DMN <sub><i>t-1</i></sub>	-0.12	0.13	-0.95 (.339)
		<b>Estradiol<sub><i>t-1</i></sub></b>	<b>1.15</b>	<b>0.19</b>	<b>6.15 (&lt;.0001)</b>
		DMN <sub><i>t-2</i></sub>	-0.01	0.13	-0.08 (.930)
		<b>Estradiol<sub><i>t-2</i></sub></b>	<b>-0.48</b>	<b>0.19</b>	<b>-2.50 (.012)</b>
<i>R</i> <sup>2</sup> = 0.67 ( <i>p</i> <.0001); RMSE = 0.58 ( <i>p</i> = .0004)					
Efficiency	Control	Constant	0.01	0.16	0.08 (.783)
		DAN <sub><i>t-1</i></sub>	-0.11	0.18	-0.60 (.562)
		<b>Estradiol<sub><i>t-1</i></sub></b>	<b>0.84</b>	<b>0.25</b>	<b>3.35 (.002)</b>
		DAN <sub><i>t-2</i></sub>	-0.10	0.18	-0.58 (.571)
		<b>Estradiol<sub><i>t-2</i></sub></b>	<b>-0.67</b>	<b>0.16</b>	<b>-2.57 (.017)</b>
<i>R</i> <sup>2</sup> = 0.37 ( <i>p</i> = .002); RMSE = 0.77 ( <i>p</i> = .023)					
Estradiol	Temporal Parietal	Constant	0.01	0.12	0.06 (.808)
		DAN <sub><i>t-1</i></sub>	-0.17	0.13	-1.29 (.207)
		<b>Estradiol<sub><i>t-1</i></sub></b>	<b>1.17</b>	<b>0.19</b>	<b>6.30 (&lt;.0001)</b>
		DAN <sub><i>t-2</i></sub>	-0.02	0.13	0.24 (.806)
		<b>Estradiol<sub><i>t-2</i></sub></b>	<b>-0.48</b>	<b>0.18</b>	<b>-2.49 (.011)</b>
<i>R</i> <sup>2</sup> = 0.68 ( <i>p</i> <.0001); RMSE = 0.57 ( <i>p</i> = .0004)					

*Note.* *p*-values empirically-derived via 10,000 iterations of nonparametric permutation testing.

<sup>223</sup> *t* = -2.57, *p* = .017). As above, Dorsal Attention efficiency had no significant effects on

<sup>224</sup> estradiol, nor were there significant autoregressive effects of the network on itself.

<sup>225</sup> The Control and Temporal Parietal networks also yielded partial support for

<sup>226</sup> time-dependent modulation of efficiency by estradiol (Control *R*<sup>2</sup> = 0.34, *p* = .039;

<sup>227</sup> Temporal Parietal *R*<sup>2</sup> = 0.36, *p* = .026). The time-lagged effects of estradiol followed the

228 trends observed above; however, the overall model fit (with respect to prediction error)  
229 was not significantly better than their empirical nulls (Control  $RMSE = 0.83, p = .133$ ;  
230 Temporal Parietal  $RMSE = 0.79, p = .057$ ). Estradiol did not explain a significant  
231 proportion of variance in efficiency for any other networks (see **Supplementary Table 2**  
232 for a complete summary of VAR models for global efficiency).

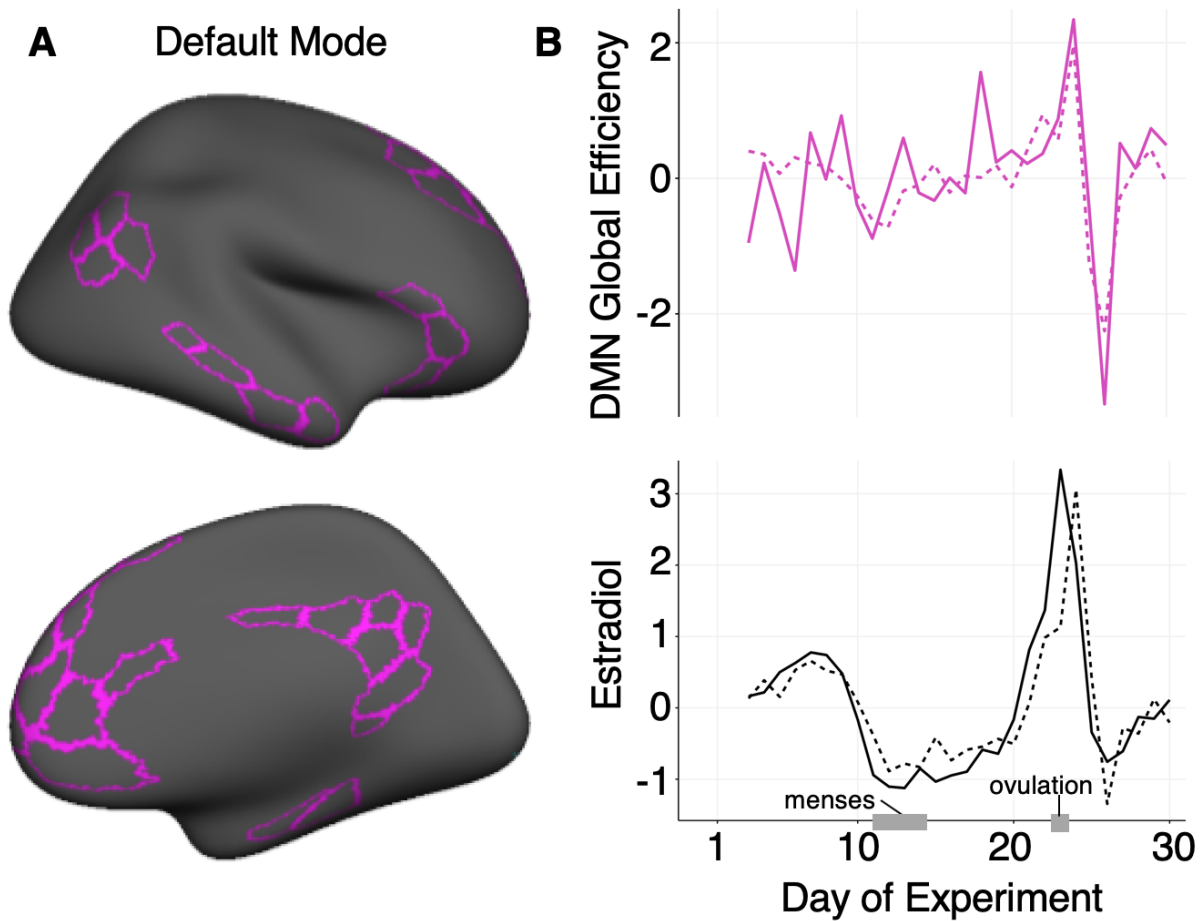


**Figure 5. Default Mode Network topology is driven by previous states of estradiol.** Observed data (solid lines) vs. VAR model fits (dotted lines) for within-network efficiency (B, right) in the Default Mode Network (A, left). The efficiency timeseries is depicted above in (B) and estradiol is plotted below. Data are in standardized units and begin at experiment day three, given the second-order VAR (lag of two days).

233

## Discussion

234 In this dense-sampling, deep-phenotyping project, a naturally-cycling female underwent  
235 resting state fMRI and venipuncture for 30 consecutive days, capturing the dynamic  
236 endocrine changes that unfold over the course of a complete menstrual cycle.

237 Time-synchronous analyses illustrate estradiol's widespread impact on cortical dynamics,  
238 spanning all but one of the networks in our parcellation. Time-lagged vector  
239 autoregressive models tested the temporal directionality of these effects, suggesting that  
240 intrinsic network dynamics are driven by recent states of estradiol, particularly with  
241 respect to within-network connectivity. Estradiol had the strongest predictive effects on  
242 the efficiency of Default Mode and Dorsal Attention Networks, with model fit being  
243 strongly driven by ovulation. In contrast to estradiol's proliferative effects, progesterone  
244 was primarily associated with reduced coherence across the whole brain. These results  
245 reveal the rhythmic nature of brain network reorganization across the human menstrual  
246 cycle.

247 The network neuroscience community has begun to probe functional networks over  
248 the timescale of weeks, months, and years to understand the extent to which brain  
249 networks vary between individuals or within an individual over time<sup>5,6,26-29</sup>. These  
250 studies indicate that functional networks are dominated by common organizational  
251 principles and stable individual features, especially in frontoparietal control regions<sup>6,7,26,28</sup>.  
252 An overlooked feature of these regions is that they are populated with estrogen and  
253 progesterone receptors and are exquisitely sensitive to major changes in sex hormone

254 concentrations<sup>11,12,15,16,30,31</sup>. Our findings demonstrate significant effects of estradiol on  
255 functional network nodes belonging to the DMN, DAN, and FCN that overlap with  
256 ER-rich regions of the brain, including medial/dorsal PFC<sup>10,32</sup>. This study merges the  
257 network neuroscience and endocrinology disciplines by demonstrating that higher-order  
258 processing systems are modulated by day-to-day changes in sex hormones over the  
259 timescale of one month.

## 260 **Sex hormones regulate brain organization across species**

261 Animal studies offer unambiguous evidence that sex steroid hormones shape the synaptic  
262 organization of the brain, particularly in regions that support higher order cognitive  
263 functions<sup>1-4,8</sup>. In rodents, estradiol increases fast-spiking interneuron excitability in deep  
264 cortical layers<sup>33</sup>. In nonhuman primates, whose reproductive cycle length is similar to  
265 humans, estradiol increases the number of synapses in PFC<sup>3</sup>. Recently, this body of work  
266 has also begun to uncover the functional significance of sinusoidal *changes* in estradiol.  
267 For example, estradiol's ability to promote PFC spinogenesis in ovariectomized animals  
268 occurs *only if* the hormone add-back regime mirrors the cyclic pattern of estradiol release  
269 typical of the macaque menstrual cycle<sup>9,34</sup>. Pairing estradiol with cyclic administration of  
270 progesterone blunts this increase in spine density<sup>34</sup>. In the hippocampus, progesterone  
271 has a similar inhibitory effect on dendritic spines, blocking the proliferative effects of  
272 estradiol 6 hours after administration<sup>1</sup>. Together, the preclinical literature suggests that  
273 progesterone antagonizes the largely proliferative effects of estradiol (for review, see  
274 Brinton and colleagues<sup>35</sup>). We observed a similar relationship, albeit at a different

275 spatiotemporal resolution, with estradiol enhancing coherence across cortical networks  
276 and progesterone diminishing it. In sum, animal studies have identified estradiol's  
277 influence on regional brain organization at the microscopic scale. Here, we show that  
278 estradiol and progesterone's influence is also evident at the mesoscopic scale of  
279 whole-brain activation, measured by spectral coherence, and macroscopic features of  
280 network topology.

281 **Resting-state network characteristics differ by cycle stage**

282 Group-based and sparser-sampling neuroimaging studies provide further support that  
283 cycle stage and sex hormones impact resting state networks<sup>13,14</sup>. Arélin and colleagues<sup>36</sup>  
284 sampled an individual every 2-3 days across four cycles and found that progesterone was  
285 associated with increased connectivity between the hippocampus, dorsolateral PFC, and  
286 the sensorimotor cortex, providing compelling evidence that inter-regional connectivity  
287 varies over the cycle. However, the sampling rate of this correlational study precluded the  
288 authors from capturing the neural effects of day-to-day changes in sex steroid hormones  
289 and from testing the temporal directionality of the effect with time-lagged models.

290 Estradiol has both rapid, non-genomic effects and slower, genomic effects on the central  
291 nervous system. For example, over the rat estrous cycle, there is a dramatic 30% increase  
292 in hippocampal spine density within the 24-hour window in which estradiol  
293 concentrations peak. Here, we sought to capture both time-synchronous (rapid) and  
294 time-lagged (delayed) effects of sex steroid hormones, sampling every 24 hours for 30  
295 consecutive days. In contrast to Arélin and colleagues, we observed robust,

296 spatially-diffuse negative relationships between progesterone and coherence across the  
297 brain, while estradiol enhanced the global efficiency of discrete networks along with  
298 between-network integration. Our results illuminate how simultaneous,  
299 time-synchronous correlations and causal, time-lagged analysis reveal unique aspects of  
300 where and how hormones exert their effect on the brain's intrinsic networks. Time  
301 synchronous analyses illustrate estrogen and progesterone's widespread influence on  
302 cortical coupling. Time-lagged models, which allowed us to examine the temporal  
303 direction of those relationships, show that estradiol is *driving* increased connectivity,  
304 particularly in DMN and DAN.

### 305 **Neurobiological interpretations of hormonal effects and future studies**

306 The following considerations could enhance the interpretation of these data. First, this  
307 study represents extensive neural phenotyping of a healthy participant with canonical  
308 hormone fluctuations over a reproductive cycle. To enrich our understanding of the  
309 relationship between sex hormones and brain function, examining network organization  
310 in a hormonally-suppressed female (i.e. an oral contraceptive user) would serve as a  
311 valuable comparison. Oral hormonal contraceptives suppress the production of ovarian  
312 hormones. If dynamic changes in estradiol are indeed *causing* increases in resting  
313 connectivity, we expect hormonally-suppressed individuals to show blunted functional  
314 brain network dynamics over time. Given the widespread use of oral hormonal  
315 contraceptives (100 million users worldwide), it is critical to determine whether sweeping

316 changes to an individual's endocrine state impacts brain states and whether this, in turn,  
317 has any bearing on cognition.

318 Second, in normally-cycling individuals, sex hormones function as  
319 proportionally-coupled *nonlinear* oscillators<sup>37</sup>. Within-person cycle variability is almost as  
320 large as between-person cycle variability, which hints that there are highly-complex  
321 hormonal interactions within this regulatory system<sup>37,38</sup>. The VAR models we have  
322 explored reveal *linear* dependencies between brain states and hormones, but other  
323 dynamical systems methods (e.g. coupled latent differential equations) may offer more  
324 biophysical validity<sup>37</sup>. Unfortunately, the current sample size precludes robust estimation  
325 of such a model. Our investigation deeply sampled a single individual across one  
326 complete cycle; future studies should enroll a larger sample of women to assess whether  
327 individual differences in hormone dynamics drive network changes.

328 Third, while coherence is theoretically robust to timing differences in the  
329 hemodynamic response function, hormones can affect the vascular system<sup>39</sup>. Therefore,  
330 changes in coherence may be due to vascular artifacts that affect the hemodynamic  
331 response in fMRI, rather than being *neurally*-relevant. Future investigations exploring the  
332 assumptions of hemodynamics in relation to sex steroid hormone concentrations will add  
333 clarity as to how the vascular system's response to hormones might influence large-scale  
334 brain function.

335 Fourth, these findings contribute to an emerging body of work on estradiol's ability  
336 to enhance the efficiency of PFC-based cortical circuits. In young women performing a

337 working memory task, PFC activity is exaggerated under low estradiol conditions and  
338 reduced under high estradiol conditions<sup>12</sup>. The same pattern is observed decades later in  
339 life: as estradiol production decreases over the menopausal transition, working  
340 memory-related PFC activity becomes more exaggerated, despite no difference in working  
341 memory performance<sup>15</sup>. Here, we show that day-to-day changes in estradiol drive the  
342 global efficiency of functional networks, with the most pronounced effects in networks  
343 with major hubs in the PFC. Together, these findings suggest that estradiol generates a  
344 neurally efficient PFC response at rest and while engaging in a cognitive task. Estradiol's  
345 action may occur by enhancing dopamine synthesis and release<sup>40</sup>. The PFC is innervated  
346 by midbrain dopaminergic neurons that form the mesocortical dopamine track<sup>41</sup>. Decades  
347 of evidence have established that dopamine signaling enhances the signal-to-noise ratio of  
348 PFC pyramidal neurons<sup>42</sup> and drives cortical efficiency<sup>43-46</sup>. In turn, estradiol enhances  
349 dopamine synthesis and release and modifies the basal firing rate of dopaminergic  
350 neurons<sup>47-49</sup>, a plausible neurobiological mechanism by which alterations in estradiol  
351 could impact cortical efficiency. Future multimodal neuroimaging studies in humans can  
352 clarify the link between estradiol's ability to stimulate dopamine release and the  
353 hormone's ability to drive cortical efficiency within PFC circuits.

354 Dense-sampling approaches to probe brain-hormone interactions could reveal  
355 organizational principles of the functional connectome previously unknown, transforming  
356 our understanding of how hormones influence brain states. Human studies implicate sex  
357 steroids in the regulation of brain structure and function, particularly within ER-rich

358 regions like the PFC and hippocampus<sup>11,12,15,16,30,31,50-52</sup>, and yet, the neuroendocrine basis  
359 of the brain's network organization remains understudied. Here, we used a network  
360 neuroscience approach to investigate how hormonal dynamics modulate the integration of  
361 functional brain networks, showing that estradiol is associated with increased coherence  
362 across broad swaths of cortex. At the network level, estradiol enhances the efficiency of  
363 most functional networks (with robust effects in DAN and DMN) and, to a lesser extent,  
364 increases between-network participation. Moving forward, this network neuroscience  
365 approach can be applied to brain imaging studies of other major neuroendocrine  
366 transitions, such as pubertal development and reproductive aging (e.g. menopause).

### 367 **Implications of hormonally regulated network dynamics for cognition**

368 An overarching goal of network neuroscience is to understand how coordinated activity  
369 within and between functional brain networks supports cognition. Increased global  
370 efficiency is thought to optimize a cognitive workspace<sup>53</sup>, while between-network  
371 connectivity may be integral for integrating top-down signals from multiple higher-order  
372 control hubs<sup>54</sup>. The dynamic reconfiguration of functional brain networks is implicated in  
373 performance across cognitive domains, including motor learning<sup>55,56</sup>, cognitive control<sup>57</sup>,  
374 and memory<sup>58</sup>. Our results demonstrate that within- and between-network connectivity  
375 of these large-scale networks at rest are hormonally regulated across the human menstrual  
376 cycle. Future studies should consider whether these network changes confer advantages  
377 to domain-general or domain-specific cognitive performance. Further, planned analyses  
378 from this dataset will incorporate task-based fMRI to determine whether the brain's

379 network architecture is hormonally regulated across the cycle when engaging in a  
380 cognitive task, or in the dynamic reconfiguration that occurs when transitioning from rest  
381 to task.

382 **Implications of hormonally regulated network dynamics for clinical**  
383 **diagnoses**

384 Clinical network neuroscience seeks to understand how large-scale brain networks differ  
385 between healthy and patient populations<sup>59,60</sup>. Disruptions in functional brain networks  
386 are implicated in a number of neurodegenerative and neuropsychiatric disorders: intrinsic  
387 connectivity abnormalities in the DMN are evident in major depressive disorder<sup>61</sup> and  
388 Alzheimer's disease<sup>62</sup>. Notably, these conditions have a sex-skewed disease prevalence:  
389 women are at twice the risk for depression and make up two-thirds of the Alzheimer's  
390 disease patient population<sup>63</sup>. Here, we show that global efficiency in the DMN and DAN  
391 are hormonally regulated, with estradiol driving increases in within-network integration.  
392 A long history of clinical evidence further implicates sex hormones in the development of  
393 mood disorders<sup>64-66</sup>. For example, the incidence of major depression increases with  
394 pubertal onset in females<sup>67</sup>, chronic use of hormonal contraceptives<sup>68</sup>, the postpartum  
395 period<sup>69</sup>, and perimenopause<sup>70</sup>. Moving forward, a network neuroscience approach might  
396 have greater success at identifying the large-scale network disturbances that underlie, or  
397 predict, the emergence of disease symptomology. Incorporating sex-dependent variables  
398 (such as endocrine status) into clinical models. This may be particularly true during  
399 periods of profound neuroendocrine change (e.g. puberty, pregnancy, menopause, and use

400 of hormone-based medications, reviewed by Taylor and colleagues<sup>71</sup>) given that these  
401 hormonal transitions are associated with a heightened risk for mood disorders.

402 **Conclusion**

403 In sum, endogenous hormone fluctuations over the reproductive cycle have a robust  
404 impact on the intrinsic network properties of the human brain. Despite over 20 years of  
405 evidence from rodent, nonhuman primate, and human studies demonstrating the  
406 tightly-coupled relationship between our endocrine and nervous systems<sup>3,72,73</sup>, the field of  
407 network neuroscience has largely overlooked how endocrine factors shape the brain. The  
408 dynamic endocrine changes that unfold over the menstrual cycle are a natural feature of  
409 half of the world's population. Understanding how these changes in sex hormones  
410 influence the large-scale functional architecture of the human brain is imperative for our  
411 basic understanding of the brain and for women's health.

412

## End Notes

413       **Acknowledgements.** This work was supported by the Brain and Behavior Research  
414       Foundation (EGJ), the California Nanosystems Institute (EGJ), the Institute for  
415       Collaborative Biotechnologies through grant W911NF-19-D-0001 from the U.S. Army  
416       Research Office (MBM), and the Rutherford B. Fett Fund (STG). Thanks to Mario Mendoza  
417       for phlebotomy and MRI assistance. We would also like to thank Courtney Kenyon,  
418       Maggie Hayes, and Morgan Fitzgerald for assistance with data collection.

419       **Author contributions.** The overall study was conceived by L.P., C.M.T., S.T.G., and  
420       E.G.J.; L.P., T.S., E.L., C.M.T., S.Y., and E.G.J. performed the experiments; data analysis  
421       strategy was conceived by T.S. and L.P. and implemented by T.S.; L.P., T.S., and E.G.J.  
422       wrote the manuscript; E.L., C.M.T., S.Y., M.B.M., and S.T.G. edited the manuscript.

423       **Data/code availability.** MRI data, code, and daily behavioral assessments will be  
424       publicly accessible upon publication.

425       **Conflict of interest.** The authors declare no competing financial interests.

426

## Methods and Materials

### 427 Participants

428 The participant (author L.P.) was a right-handed Caucasian female, aged 23 years for  
429 duration of the study. The participant had no history of neuropsychiatric diagnosis,  
430 endocrine disorders, or prior head trauma. She had a history of regular menstrual cycles  
431 (no missed periods, cycle occurring every 26-28 days) and had not taken hormone-based  
432 medication in the prior 12 months. The participant gave written informed consent and the  
433 study was approved by the University of California, Santa Barbara Human Subjects  
434 Committee.

### 435 Study design

436 The participant underwent daily testing for 30 consecutive days, with the first test session  
437 determined independently of cycle stage for maximal blindness to hormone status. The  
438 participant began each test session with a daily questionnaire (see **Behavioral**  
439 **assessments**), followed by an immersive reality spatial navigation task (not reported here)  
440 (**Figure 6**). Time-locked collection of serum and whole blood started each day at 10:00am,  
441 when the participant gave a blood sample. Endocrine samples were collected, at  
442 minimum, after two hours of no food or drink consumption (excluding water). The  
443 participant refrained from consuming caffeinated beverages before each test session. The  
444 MRI session lasted one hour and consisted of structural and functional MRI sequences.

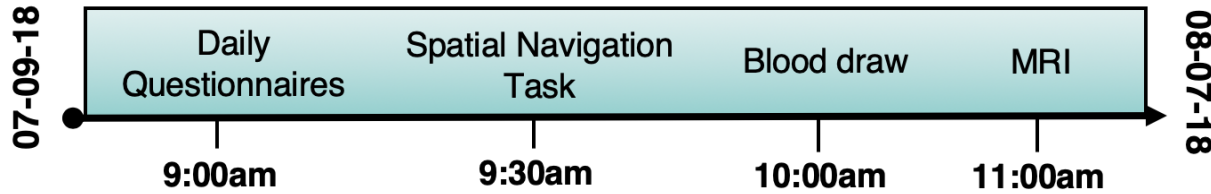


**Figure 6. Timeline of data collection for the 30 experiment sessions.** Endocrine and MRI assessments were collected at the same time each day to minimize time-of-day effects.

#### 445 **Behavioral assessments**

446 To monitor state-dependent mood and lifestyle measures over the cycle, the following  
447 scales (adapted to reflect the past 24 hours) were administered each morning: Perceived  
448 Stress Scale (PSS)<sup>74</sup>, Pittsburgh Sleep Quality Index (PSQI)<sup>75</sup>, State-Trait Anxiety Inventory  
449 for Adults (STAI)<sup>76</sup>, and Profile of Mood States (POMS)<sup>77</sup>. We observed very few  
450 significant relationships between hormone and state-dependent measures following an  
451 FDR-correction for multiple comparisons ( $q < .05$ )—and critically, none of these  
452 state-dependent factors were associated with estradiol (**Figure 7A**). The participant had  
453 moderate levels of anxiety as determined by STAI reference ranges; however, all other  
454 measures fell within the ‘normal’ standard range (**Figure 7B**).

#### 455 **Endocrine procedures**

456 A licensed phlebotomist inserted a saline-lock intravenous line into the dominant or  
457 non-dominant hand or forearm daily to evaluate hypothalamic-pituitary-gonadal axis  
458 hormones, including serum levels of gonadal hormones (17 $\beta$ -estradiol, progesterone and  
459 testosterone) and the pituitary gonadotropins luteinizing hormone (LH) and follicle  
460 stimulating hormone (FSH). One 10cc mL blood sample was collected in a vacutainer SST

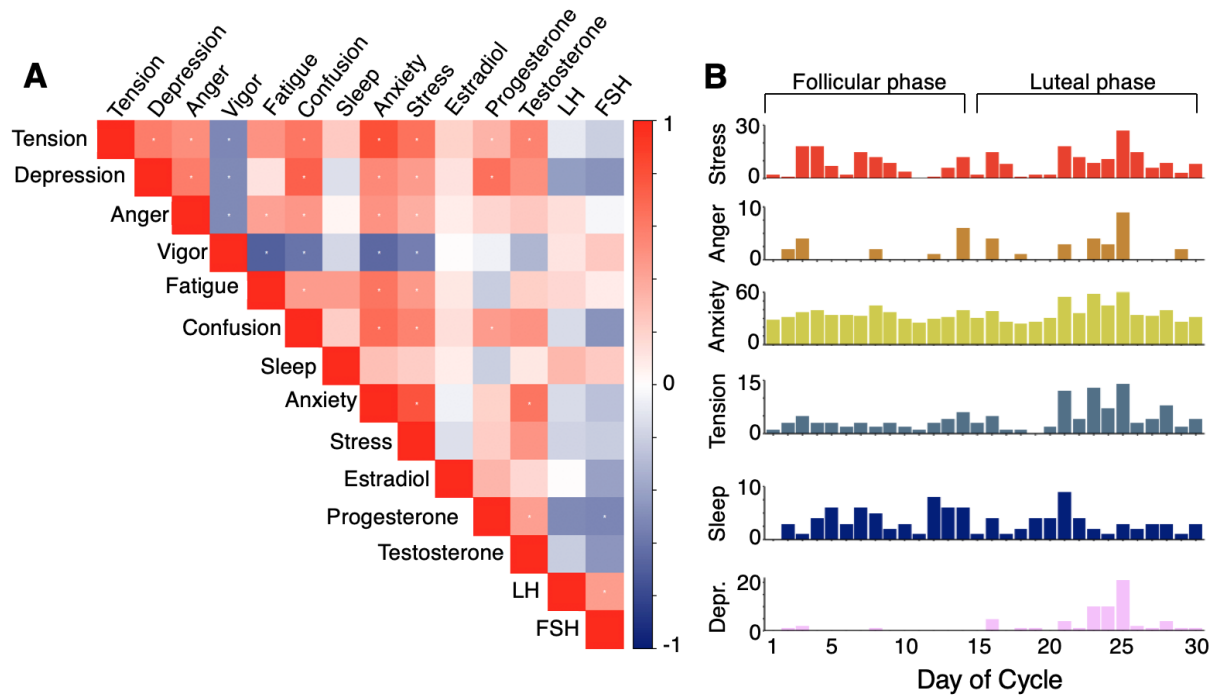


**Figure 7. Behavioral variation across the 30 day experiment.** (A) Correlation plot showing relationships between mood, lifestyle measures, and sex steroid hormone concentrations. Cooler cells indicate negative correlations, warm cells indicate positive correlations, and white cells indicate no relationship. Asterisks indicate significant correlations after FDR correction ( $q < .05$ ). (B) Mood and lifestyle measures vary across the cycle. 'Day 1' indicates first day of menstruation, *not* first day of experiment. Abbreviations: LH, Lutenizing hormone; FSH, Follicle-stimulating hormone.

461 (BD Diagnostic Systems) each session. The sample clotted at room temperature for 45 min  
462 until centrifugation ( $2,000 \times g$  for 10 minutes) and were then aliquoted into three 1 mL  
463 microtubes. Serum samples were stored at  $-20^{\circ} C$  until assayed. Serum concentrations  
464 were determined via liquid chromatography-mass spectrometry (for all steroid hormones)  
465 and immunoassay (for all gonadotropins) at the Brigham and Women's Hospital Research  
466 Assay Core. Assay sensitivities, dynamic range, and intra-assay coefficients of variation  
467 (respectively) were as follows: estradiol, 1 pg/mL, 1–500 pg/mL, < 5% relative standard  
468 deviation (RSD); progesterone, 0.05 ng/mL, 0.05–10 ng/mL, 9.33% RSD; testosterone, 1.0

469 ng/dL, 1–2000 ng/dL, < 4% *RSD*; FSH and LH levels were determined via  
470 chemiluminescent assay (Beckman Coulter). The assay sensitivity, dynamic range, and the  
471 intra-assay coefficient of variation were as follows: FSH, 0.2 mIU/mL, 0.2–200 mIU/mL,  
472 3.1–4.3%; LH, 0.2 mIU/mL, 0.2–250 mIU/mL, 4.3–6.4%.

## 473 fMRI acquisition and preprocessing

474 The participant underwent a daily magnetic resonance imaging scan on a Siemens 3T  
475 Prisma scanner equipped with a 64-channel phased-array head coil. First, high-resolution  
476 anatomical scans were acquired using a  $T_1$ -weighted magnetization prepared rapid  
477 gradient echo (MPRAGE) sequence (TR = 2500 ms, TE = 2.31 ms, TI = 934 ms, flip angle =  
478 7°; 0.8 mm thickness) followed by a gradient echo fieldmap (TR = 758 ms, TE<sub>1</sub> = 4.92 ms,  
479 TE<sub>2</sub> = 7.38 ms, flip angle = 60°). Next, the participant completed a 10-minute resting-state  
480 fMRI scan using a  $T_2^*$ -weighted multiband echo-planar imaging (EPI) sequence sensitive  
481 to the blood oxygenation level-dependent (BOLD) contrast (TR = 720 ms, TE = 37 ms, flip  
482 angle = 56°, multiband factor = 8; 72 oblique slices, voxel size = 2 mm<sup>3</sup>). In an effort to  
483 minimize motion, the head was secured with a custom, 3D-printed foam head case  
484 (<https://caseforge.co/>) (days 8–30). Overall motion (mean framewise  
485 displacement) was negligible (**Supplementary Figure 3**), with fewer than 130 microns of  
486 motion on average each day. Importantly, mean framewise displacement was also not  
487 correlated with estradiol concentrations (Spearman  $r = -0.06, p = .758$ ).

488 Initial preprocessing was performed using the Statistical Parametric Mapping 12  
489 software (SPM12, Wellcome Trust Centre for Neuroimaging, London) in Matlab.

490 Functional data were realigned and unwarped to correct for head motion and the mean  
491 motion-corrected image was coregistered to the high-resolution anatomical image. All  
492 scans were then registered to a subject-specific anatomical template created using  
493 Advanced Normalization Tools' (ANTs) multivariate template construction  
494 (**Supplementary Figure 4**). A 4 mm full-width at half-maximum (FWHM) isotropic  
495 Gaussian kernel was subsequently applied to smooth the functional data. Further  
496 preparation for resting-state functional connectivity was implemented using in-house  
497 Matlab scripts. Global signal scaling (median = 1,000) was applied to account for transient  
498 fluctuations in signal intensity across space and time, and voxelwise timeseries were  
499 linearly detrended. Residual BOLD signal from each voxel was extracted after removing  
500 the effects of head motion and five physiological noise components (CSF + white matter  
501 signal). Motion was modeled based on the Friston-24 approach, using a Volterra  
502 expansion of translational/rotational motion parameters, accounting for autoregressive  
503 and nonlinear effects of head motion on the BOLD signal<sup>78</sup>. All nuisance regressors were  
504 detrended to match the BOLD timeseries.

## 505 **Functional connectivity estimation**

506 Functional network nodes were defined based on a 400-region cortical parcellation<sup>25</sup> and  
507 15 regions from the Harvard-Oxford subcortical atlas  
508 (<http://www.fmrib.ox.ac.uk/fsl/>). For each day, a summary timecourse was  
509 extracted per node by taking the first eigenvariate across functional volumes<sup>79</sup>. These  
510 regional timeseries were then decomposed into several frequency bands using a maximal

511 overlap discrete wavelet transform. Low-frequency fluctuations in wavelets 3–6  
512 ( $\sim 0.01$ –0.17 Hz) were selected for subsequent connectivity analyses<sup>80</sup>. Finally, we  
513 estimated the spectral association between regional timeseries using magnitude-squared  
514 coherence: this yielded a  $415 \times 415$  functional association matrix each day, whose  
515 elements indicated the strength of functional connectivity between all pairs of nodes  
516 (FDR-thresholded at  $q < .05$ ).

## 517 Statistical analysis

518 First, we assessed time-synchronous variation in functional connectivity associated with  
519 estradiol and progesterone through a standardized regression analysis. Data were  
520  $Z$ -transformed and edgewise coherence was regressed against hormonal timeseries to  
521 capture day-by-day variation in connectivity relative to hormonal fluctuations. For each  
522 model, we computed robust empirical null distributions of test-statistics via 10,000  
523 iterations of nonparametric permutation testing—while this process has been shown to  
524 adequately approximate false positive rates of 5%<sup>81</sup>, we elected to report only those edges  
525 surviving a conservative threshold of  $p < .001$  to avoid over-interpretation of whole-brain  
526 effects.

527 Next, we sought to capture *causal* linear dependencies between hormonal fluctuations  
528 and network connectivity over time using vector autoregressive (VAR) models. A given  
529 VAR model takes a set of variables at time,  $t$ , and simultaneously regresses them against  
530 previous (time-lagged) states of themselves and each other. For consistency, we only  
531 considered second-order VAR models, given a fairly reliable first zero-crossing of

532 brain/hormone autocovariance at lag two. Fit parameters for each VAR therefore reflect  
533 the following general form:

$$Brain_t = b_{1,0} + b_{1,1}Brain_{t-1} + b_{1,2}Estradiol_{t-1} + b_{1,3}Brain_{t-2} + b_{1,4}Estradiol_{t-2} + \epsilon_t$$

$$Estradiol_t = b_{2,0} + b_{2,1}Brain_{t-1} + b_{2,2}Estradiol_{t-1} + b_{2,3}Brain_{t-2} + b_{2,4}Estradiol_{t-2} + \epsilon_t \quad (1)$$

534 With respect to brain states, we modeled both edgewise coherence and factors related  
535 to macroscale network topologies. Specifically, we computed measures of *between-network*  
536 integration (the participation coefficient; i.e. the average extent to which network nodes  
537 are communicating with other networks over time) and *within-network* integration (global  
538 efficiency, quantifying the ostensible ease of information transfer across nodes inside a  
539 given network). Regardless of brain measure, each VAR was estimated similarly to the  
540 time-synchronous analyses described above: data were *Z*-scored, models were fit, and all  
541 effects were empirically-thresholded against 10,000 iterations of nonparametric  
542 permutation testing.

543 Finally, for each set of edgewise models (time-synchronous and time-lagged), we  
544 attempted to disentangle both the general *direction* of hormone-related associations and  
545 whether certain networks were more or less *susceptible* to hormonal fluctuations. Toward  
546 that end, we estimated *nodal association strengths* per graph theory's treatment of signed,  
547 weighted networks—that is, positive and negative association strengths were computed  
548 independently for each node by summing the positive and negative edges linked to them  
549 (after empirical thresholding), respectively. We then simply assessed mean association  
550 strengths across the various networks in our parcellation.

551 Here, networks were defined by grouping the subnetworks of the 17-network  
552 Schaefer parcellation, such that (for example), the A, B, and C components of the Default  
553 Mode Network were treated as one network. We chose this due to the presence of a  
554 unique Temporal Parietal Network in the 17-network partition, which is otherwise  
555 subsumed by several other networks (Default Mode, Salience/Ventral Attention, and  
556 SomatoMotor) in the 7-network partition. The subcortical nodes of the Harvard-Oxford  
557 atlas were also treated as their own network, yielding a total of nine networks. These  
558 definitions were subsequently used for computation of participation coefficients and  
559 global efficiencies in network-level VAR models.

560 **Brain data visualization**

561 Statistical maps of edgewise coherence v. hormones were visualized using the Surf Ice  
562 software (<https://www.nitrc.org/projects/surface/>).

## References

- [1] Woolley CS, McEwen BS (1993) Roles of estradiol and progesterone in regulation of hippocampal dendritic spine density during the estrous cycle in the rat. *J. Comp. Neurol.* 336(2):293–306.
- [2] Frick KM, Kim J, Tuscher JJ, Fortress AM (2015) Sex steroid hormones matter for learning and memory: Estrogenic regulation of hippocampal function in male and female rodents. *Learn. Mem.* 22(9):472–493.
- [3] Hara Y, Waters EM, McEwen BS, Morrison JH (2015) Estrogen effects on cognitive and synaptic health over the lifecourse. *Physiol. Rev.* 95(3):785–807.
- [4] Galea LAM, Frick KM, Hampson E, Sohrabji F, Choleris E (2017) Why estrogens matter for behavior and brain health. *Neurosci. Biobehav. Rev.* 76(Pt B):363–379.
- [5] Poldrack RA, et al. (2015) Long-term neural and physiological phenotyping of a single human. *Nat. Commun.* 6:8885.
- [6] Gordon EM, et al. (2017) Precision functional mapping of individual human brains. *Neuron* 95(4):791–807.
- [7] Gratton C, et al. (2018) Functional brain networks are dominated by stable group and individual factors, not cognitive or daily variation. *Neuron* 98(2):439–452.
- [8] Frick KM, Kim J, Koss WA (2018) Estradiol and hippocampal memory in female and male rodents. *Curr. Opin. Behav. Sci.* 23:65–74.
- [9] Hao J, et al. (2006) Estrogen alters spine number and morphology in prefrontal cortex of aged female rhesus monkeys. *J. Neurosci.* 26(9):2571–2578.
- [10] Wang ACJ, Hara Y, Janssen WGM, Rapp PR, Morrison JH (2010) Synaptic estrogen receptor-alpha levels in prefrontal cortex in female rhesus monkeys and their correlation with cognitive performance. *J. Neurosci.* 30(38):12770–12776.

- [11] Berman KF, et al. (1997) Modulation of cognition-specific cortical activity by gonadal steroids: a positron-emission tomography study in women. *Proc. Natl. Acad. Sci. U.S.A.* 94(16):8836–8841.
- [12] Jacobs E, D'Esposito M (2011) Estrogen shapes dopamine-dependent cognitive processes: Implications for women's health. *J. Neurosci.* 31(14):5286–5293.
- [13] Petersen N, Kilpatrick LA, Goharzad A, Cahill L (2014) Oral contraceptive pill use and menstrual cycle phase are associated with altered resting state functional connectivity. *Neuroimage* 90:24–32.
- [14] Lisofsky N, et al. (2015) Hippocampal volume and functional connectivity changes during the female menstrual cycle. *Neuroimage* 118:154–162.
- [15] Jacobs EG, et al. (2016) Reorganization of functional networks in verbal working memory circuitry in early midlife: The impact of sex and menopausal status. *Cereb. Cortex* 27(5):2857–2870.
- [16] Jacobs EG, et al. (2016) Impact of sex and menopausal status on episodic memory circuitry in early midlife. *J. Neurosci.* 36(39):10163–10173.
- [17] Sheppard PAS, Choleris E, Galea LAM (2019) Structural plasticity of the hippocampus in response to estrogens in female rodents. *Mol. Brain* 12(1):22.
- [18] Warren SG, Juraska JM (1997) Spatial and nonspatial learning across the rat estrous cycle. *Behav. Neurosci.* 111(2):259–266.
- [19] Hampson E, Levy-Cooperman N, Korman JM (2014) Estradiol and mental rotation: Relation to dimensionality, difficulty, or angular disparity? *Horm. Behav.* 65(3):238–248.
- [20] Kim J, Frick KM (2017) Distinct effects of estrogen receptor antagonism on object recognition and spatial memory consolidation in ovariectomized mice. *Psychoneuroendocrinology* 85:110–114.

- [21] Hjelmervik H, Hausmann M, Osnes B, Westerhausen R, Specht K (2014) Resting states are resting traits—an fmri study of sex differences and menstrual cycle effects in resting state cognitive control networks. *PLoS One* 9(7):e103492.
- [22] De Bondt T, et al. (2015) Stability of resting state networks in the female brain during hormonal changes and their relation to premenstrual symptoms. *Brain Res.* 1624:275–285.
- [23] Syan SK, et al. (2017) Influence of endogenous estradiol, progesterone, allopregnanolone, and dehydroepiandrosterone sulfate on brain resting state functional connectivity across the menstrual cycle. *Fertil. Steril.* 107(5):1246–1255.
- [24] Leiva R, Bouchard T, Boehringer H, Abulla S, Ecochard R (2015) Random serum progesterone threshold to confirm ovulation. *Steroids* 101:125–129.
- [25] Schaefer A, et al. (2018) Local-global parcellation of the human cerebral cortex from intrinsic functional connectivity mri. *Cereb. Cortex* 28(9):3095–3114.
- [26] Finn ES, et al. (2015) Functional connectome fingerprinting: Identifying individuals using patterns of brain connectivity. *Nat. Neurosci.* 18(11):1664–1671.
- [27] Betzel RF, et al. (2019) The community structure of functional brain networks exhibits scale-specific patterns of inter- and intra-subject variability. *Neuroimage*.
- [28] Horien C, Shen X, Scheinost D, Constable RT (2019) The individual functional connectome is unique and stable over months to years. *Neuroimage* 189:676–687.
- [29] Seitzman BA, et al. (2019) Trait-like variants in human functional brain networks. *Proc. Natl. Acad. Sci. U.S.A.* 116(45):22851–22861.
- [30] Hampson E, Morley EE (2013) Estradiol concentrations and working memory performance in women of reproductive age. *Psychoneuroendocrinology* 38(12):2897–2904.

- [31] Shanmugan S, Epperson CN (2014) Estrogen and the prefrontal cortex: towards a new understanding of estrogen's effects on executive functions in the menopause transition. *Hum. Brain. Mapp.* 35(3):847–865.
- [32] Yeo BTT, et al. (2011) The organization of the human cerebral cortex estimated by intrinsic functional connectivity. *J. Neurophysiol.* 106(3):1125–1165.
- [33] Clemens AM, et al. (2019) Estrus-cycle regulation of cortical inhibition. *Curr. Biol.* 29(4):605–615.
- [34] Ohm DT, et al. (2012) Clinically relevant hormone treatments fail to induce spinogenesis in prefrontal cortex of aged female rhesus monkeys. *J. Neurosci.* 32(34):11700–11705.
- [35] Brinton RD, et al. (2008) Progesterone receptors: form and function in brain. *Front. Neuroendocrinol.* 29(2):313–339.
- [36] Arelin K, et al. (2015) Progesterone mediates brain functional connectivity changes during the menstrual cycle-a pilot resting state mri study. *Front. Neurosci.* 9:44.
- [37] Boker SM, Neale MC, Klump KL (2014) *A differential equations model for the ovarian hormone cycle.*, eds. Molenaar PC, Lerner R, Newell K. (Guilford Press, New York), pp. 369–391.
- [38] Fehring RJ, Schneider M, Raviele K (2006) Variability in the phases of the menstrual cycle. *J. Obstet. Gynecol. Neonatal. Nurs.* 35(3):376–384.
- [39] Krause DN, Duckles SP, Pelligrino DA (2006) Influence of sex steroid hormones on cerebrovascular function. *J. Appl. Physiol.* 101(4):1252–1261.
- [40] Creutz LM, Kritzer MF (2002) Estrogen receptor-beta immunoreactivity in the midbrain of adult rats: regional, subregional, and cellular localization in the a10, a9, and a8 dopamine cell groups. *J. Comp. Neurol.* 446(3):288–300.

- [41] Kritzer MF, Creutz LM (2008) Region and sex differences in constituent dopamine neurons and immunoreactivity for intracellular estrogen and androgen receptors in mesocortical projections in rats. *J. Neurosci.* 28(38):9525–9535.
- [42] Williams GV, Goldman-Rakic PS (1995) Modulation of memory fields by dopamine d1 receptors in prefrontal cortex. *Nature* 376(6541):572–575.
- [43] Cai JX, Arnsten AF (1997) Dose-dependent effects of the dopamine d1 receptor agonists a77636 or skf81297 on spatial working memory in aged monkeys. *J. Pharmacol. Exp. Ther.* 283(1):183–189.
- [44] Granon S, et al. (2000) Enhanced and impaired attentional performance after infusion of d1 dopaminergic receptor agents into rat prefrontal cortex. *J. Neurosci.* 20(3):1208–1215.
- [45] Gibbs SEB, D'Esposito M (2005) Individual capacity differences predict working memory performance and prefrontal activity following dopamine receptor stimulation. *Cogn. Affect. Behav. Neurosci.* 5(2):212–221.
- [46] Vijayraghavan S, Wang M, Birnbaum SG, Williams GV, Arnsten AFT (2007) Inverted-u dopamine d1 receptor actions on prefrontal neurons engaged in working memory. *Nat. Neurosci.* 10(3):376–384.
- [47] Thompson TL, Moss RL (1994) Estrogen regulation of dopamine release in the nucleus accumbens: genomic- and nongenomic-mediated effects. *J. Neurochem.* 62(5):1750–1756.
- [48] Pasqualini C, Olivier V, Guibert B, Frain O, Leviel V (1995) Acute stimulatory effect of estradiol on striatal dopamine synthesis. *J. Neurochem.* 65(4):1651–1657.
- [49] Becker JB (1990) Estrogen rapidly potentiates amphetamine-induced striatal dopamine release and rotational behavior during microdialysis. *Neurosci. Lett.* 118(2):169–171.
- [50] Jacobs EG, et al. (2015) 17beta-estradiol differentially regulates stress circuitry activity in healthy and depressed women. *Neuropsychopharmacology* 40(3):566–576.

- [51] Girard R, et al. (2017) Hormone therapy at early post-menopause increases cognitive control-related prefrontal activity. *Sci. Rep.* 7:44917.
- [52] Zeydan B, et al. (2019) Association of bilateral salpingo-oophorectomy before menopause onset with medial temporal lobe neurodegeneration. *JAMA Neurol.* 76(1):95–100.
- [53] Bullmore ET, Bassett DS (2011) Brain graphs: graphical models of the human brain connectome. *Annu. Rev. Clin. Psychol.* 7:113–140.
- [54] Gratton C, Sun H, Petersen SE (2018) Control networks and hubs. *Psychophysiology* 55(3).
- [55] Bassett DS, et al. (2011) Dynamic reconfiguration of human brain networks during learning. *Proc. Natl. Acad. Sci. U.S.A.* 108(18):7641–7646.
- [56] Mattar MG, et al. (2018) Predicting future learning from baseline network architecture. *Neuroimage* 172:107–117.
- [57] Seeley WW, et al. (2007) Dissociable intrinsic connectivity networks for salience processing and executive control. *J. Neurosci.* 27(9):2349–2356.
- [58] Fornito A, Harrison BJ, Zalesky A, Simons JS (2012) Competitive and cooperative dynamics of large-scale brain functional networks supporting recollection. *Proc. Natl. Acad. Sci. U.S.A.* 109(31):12788–12793.
- [59] Fox MD, Greicius M (2010) Clinical applications of resting state functional connectivity. *Front. Syst. Neurosci.* 4:19.
- [60] Hallquist MN, Hillary FG (2019) Graph theory approaches to functional network organization in brain disorders: A critique for a brave new small-world. *Netw. Neurosci.* 3(1):1–26.
- [61] Greicius MD, et al. (2007) Resting-state functional connectivity in major depression: Abnormally increased contributions from subgenual cingulate cortex and thalamus. *Biol. Psychiatry* 62(5):429–437.

- [62] Buckner RL, et al. (2009) Cortical hubs revealed by intrinsic functional connectivity: mapping, assessment of stability, and relation to alzheimer's disease. *J. Neurosci.* 29(6):1860–1873.
- [63] Nebel RA, et al. (2018) Understanding the impact of sex and gender in alzheimer's disease: A call to action. *Alzheimers Dement.* 14(9):1171–1183.
- [64] Plotsky PM, Owens MJ, Nemeroff CB (1998) Psychoneuroendocrinology of depression: hypothalamic-pituitary-adrenal axis. *Psychiatr. Clin. North. Am.* 21(2):293–307.
- [65] Young EA, Korszun A (2002) The hypothalamic-pituitary-gonadal axis in mood disorders. *Endocrinol. Metab. Clin. North. Am.* 31(1):63–78.
- [66] Rubinow DR, Schmidt PJ (2006) Gonadal steroid regulation of mood: the lessons of premenstrual syndrome. *Front. Neuroendocrinol.* 27(2):210–216.
- [67] Angold A, Costello EJ (2006) Puberty and depression. *Child Adolesc. Psychiatr. Clin. N. Am.* 15(4):919–937.
- [68] Young EA, et al. (2007) Influences of hormone-based contraception on depressive symptoms in premenopausal women with major depression. *Psychoneuroendocrinology* 32(7):843–853.
- [69] Bloch M, et al. (2000) Effects of gonadal steroids in women with a history of postpartum depression. *Am. J. Psychiatry* 157(6):924–930.
- [70] Schmidt PJ, Rubinow DR (2009) Sex hormones and mood in the perimenopause. *Ann. N. Y. Acad. Sci.* 1179:70–85.
- [71] Taylor CM, Pritschet L, Yu S, Jacobs EG (2019) Applying a women's health lens to the study of the aging brain. *Front. Hum. Neurosci.* 13:224.
- [72] McEwen BS (2018) Redefining neuroendocrinology: Epigenetics of brain-body communication over the life course. *Front. Neuroendocrinol.* 49:8–30.

- [73] Beltz AM, Moser JS (2019) Ovarian hormones: A long overlooked but critical contributor to cognitive brain structures and function. *Ann N Y Acad Sci.*
- [74] Cohen S, Kamarck T, Mermelstein R (1983) A global measure of perceived stress. *J. Health. Soc. Behav.* 24(4):385–396.
- [75] Buysse DJ, Reynolds CF, Monk TH, Berman SR, Kupfer DJ (1989) The pittsburgh sleep quality index: a new instrument for psychiatric practice and research. *Psychiatry Res.* 28(2):193–213.
- [76] Spielberger CD, Vagg PR (1984) Psychometric properties of the STAI: A reply to ramanaiah, franzen, and schill. *J. Pers. Assess.* 48(1):95–97.
- [77] Pollock V, Cho DW, Reker D, Volavka J (1979) Profile of mood states: the factors and their physiological correlates. *J. Nerv. Ment. Dis.* 167(10):612–614.
- [78] Friston KJ, Williams S, Howard R, Frackowiak RS, Turner R (1996) Movement-related effects in fmri time-series. *Magn. Reson. Med.* 35(3):346–355.
- [79] Friston KJ, Rotshtein P, Geng JJ, Sterzer P, Henson RN (2006) A critique of functional localisers. *Neuroimage* 30(4):1077–1087.
- [80] Patel AX, Bullmore ET (2016) A wavelet-based estimator of the degrees of freedom in denoised fmri time series for probabilistic testing of functional connectivity and brain graphs. *Neuroimage* 142:14–26.
- [81] Eklund A, Nichols TE, Knutsson H (2016) Cluster failure: Why fmri inferences for spatial extent have inflated false-positive rates. *Proc. Natl. Acad. Sci. U.S.A.* 113(28):7900–7905.